Hindawi Publishing Corporation
ISRN Optics
Volume 2013, Article ID 946832, 7 pages
http://dx.doi.org/10.1155/2013/946832

Research Article

Admittance Loci Based Design of a Plasmonic Structure Using Ag-Au Bimetallic Alloy Film

Kaushik Brahmachari and Mina Ray

Department of Applied Optics and Photonics, University of Calcutta, 92 Acharya Prafulla Chandra Road, Kolkata 700 009, India

Correspondence should be addressed to Mina Ray; mraphy@caluniv.ac.in

Received 3 October 2013; Accepted 14 November 2013

Academic Editors: A. K. Dharmadhikari, J. M. Girkin, B. D. Gupta, I. S. Moreno, and K. Panajotov

A theoretical study based on the use of admittance loci method in the design of surface plasmon resonance (SPR) based structure using Ag-Au bimetallic alloy film of different alloy fractions and nanoparticle sizes has been reported along with some interesting performance related simulated results at 633 nm wavelength. The sensitivity and other performance parameter issues of the structure based on the choice of correct alloy fraction and nanoparticle size of Ag-Au bimetallic alloy film have also been discussed giving due importance to the dynamic range of the designed structure.

1. Introduction

Surface plasmon resonance (SPR) occurs due to the interaction of the p-polarized incident light with surface plasmon wave which propagates along metal-dielectric interface. The basic prism based configurations of SPR device were proposed earlier for observing surface plasmon resonance [1, 2]. SPR is a very useful technique for determining small change in refractive index (RI) of sensing sample at metal-sample interface. The sensing capability of SPR phenomenon was first reported for gas detection and biosensing [3]. A theoretical investigation on sensitivity comparison of prism and grating coupler based SPR sensors in angular and wavelength interrogation modes has been reported by Homola et al. [4]. Surface plasmon excitation in infrared region is very advantageous for sensing purposes. Surface plasmon excitation in infrared region involves the use of chalcogenide and silicon as coupling prism materials. Works on modeling of chalcogenide and silicon prism based surface plasmon resonance sensor for chemical sensing using infrared light have been reported earlier [5, 6]. An experimental work on surface plasmon resonance using various geometrical configurations of metal-dielectric interface has also been reported [7]. Admittance loci method has been used in thin film modeling [8] and design of SPR based devices [9–12]. Prism material dependency as well as sensing application of SPR based on admittance loci analysis has been reported earlier [13, 14]. Gupta and Kondoh have worked on tuning and sensitivity enhancement of SPR sensor [15]. Studies on the performance of SPR sensor using bimetallic alloy films have been reported earlier [16–18]. Some works on performance of fiber optic sensor using bimetallic alloy films have been reported [19, 20].

In the present work, admittance loci method has been used to design and analyze a plasmonic structure concerned with SPR based sensing with the main emphasis being given to the role played by alloy fraction and also the nanoparticle size in Ag-Au bimetallic alloy film at 633 nm wavelength. The advantage of using Ag-Au bimetallic alloy film is that gold (Au) ensures higher chemical stability while eliminating oxidation problems of silver (Ag). Thus, the higher sensitivity of Au and higher detection accuracy of Ag can both be simultaneously utilized in a single plasmonic structure.

2. Mathematical Background

A plasmonic structure can be designed using admittance loci technique. In this technique, the admittance of a plasmonic structure is considered, which starts from the sample and ends at the front surface of the structure. Figure 1 represents a plasmonic structure consisting of SF10 glass prism, Ag-Au

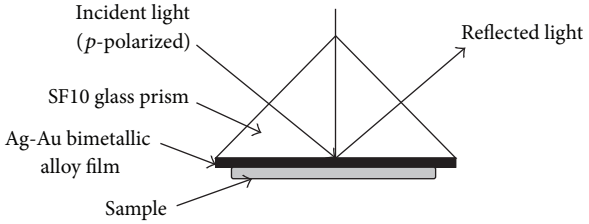

Figure 1: Schematic diagram of plasmonic structure with bimetallic (Ag-Au) alloy film.

bimetallic alloy film, and sample with refractive indices represented by n_{pr}, n_m, and n_{sample}, respectively.

The dielectric constant of any metal can be calculated using Drude model as follows:

$$\varepsilon_m(\lambda) = \varepsilon_{mr} + i\varepsilon_{mi} = 1 - \frac{\lambda^2\lambda_c}{\lambda_p^2(\lambda_c + i\lambda)}. \tag{1}$$

The collision wavelength is given by

$$\frac{1}{\lambda_c\left(R_{\text{particle}}\right)} = \frac{1}{\lambda_c(\text{bulk})} + \frac{v_f}{2\pi c R_{\text{particle}}}, \tag{2}$$

where λ_p, λ_c, and λ_c (bulk) are the plasma wavelength, collision wavelength, and bulk collision wavelength, respectively. Whereas c is the velocity of light in free space, v_f is the Fermi velocity and R_{particle} is the size of the metal nanoparticle. The values of plasma wavelength and bulk collision wavelength of different metals, namely, Au, Ag, are taken from the literature [16].

The average dielectric constant of bimetallic Ag-Au alloy film can be written as

$$\varepsilon_{\text{alloy}}(\lambda) = x\varepsilon_{\text{Ag}}(\lambda) + (1-x)\varepsilon_{\text{Au}}(\lambda), \tag{3}$$

where x is the alloy fraction and ε_{Ag}, ε_{Au} are the dielectric constants of Ag and Au, respectively.

The phase introduced by the bimetallic alloy film of thickness d_m is given by

$$\delta_m = \left(\frac{2\pi}{\lambda}\right) d_m\left(n_m^2 - k_m^2 - n_{pr}^2\sin^2\theta_i - 2in_mk_m\right)^{1/2}, \tag{4}$$

where n_m and k_m are the real and imaginary part of the complex refractive index of the bimetallic alloy film, n_{pr} is the refractive index of incident medium (SF10 glass prism as in this case), and λ is the wavelength of incident light.

The characteristic matrix of bimetallic alloy film is given by

$$\begin{bmatrix} B \\ C \end{bmatrix} = \begin{bmatrix} \cos\delta_m & \dfrac{i\sin\delta_m}{\eta_m^p} \\ i\eta_m^p\sin\delta_m & \cos\delta_m \end{bmatrix} \begin{bmatrix} 1 \\ \eta_{\text{sample}}^p \end{bmatrix}, \tag{5}$$

where B and C are the normalized electric and magnetic fields at prism-bimetallic alloy film interface, using which the properties of the bimetallic alloy film can be studied.

For bimetallic alloy film, the modified admittances are given by

$$\eta_m^s = \frac{\left(n_m^2 - k_m^2 - n_{pr}^2\sin^2\theta_i - 2in_mk_m\right)^{1/2}}{\cos\theta_i}, \qquad \eta_m^p = \frac{\left(n_m - ik_m\right)^2}{\eta_m^s}, \tag{6}$$

where the superscripts s and p denote polarization states of the incident light.

For sample, the modified admittance is given by

$$\eta_{\text{sample}}^p = \frac{y_{\text{sample}}\cos\theta_i}{\cos\theta_{\text{sample}}}, \tag{7}$$

where $y_{\text{sample}} = n_{\text{sample}}y_f$ is the optical admittance of the sample, n_{sample} is the refractive index of the sample, y_f is the free space optical admittance, and θ_{sample} is the angle corresponding to the sample.

So we can write the admittance of a plasmonic structure as

$$Y = \frac{C}{B} = \frac{\eta_{\text{sample}}^p\cos\delta_m + i\eta_m^p\sin\delta_m}{\cos\delta_m + i\left(\eta_{\text{sample}}^p/\eta_m^p\right)\sin\delta_m}. \tag{8}$$

The reflectance of a plasmonic structure is given by

$$R = \left(\frac{\eta_{pr} - Y}{\eta_{pr} + Y}\right)\left(\frac{\eta_{pr} - Y}{\eta_{pr} + Y}\right)^*. \tag{9}$$

The performance of a plasmonic structure can be visualized by plotting isoreflectance contours in the admittance diagram. These contours are the circles with centers on real axis, centers and radii being given by $((\eta_{pr}((1+R)/(1-R))), 0)$ and $2\eta_{pr}R^{1/2}/(1-R)$, where R is the reflectance and η_{pr} is the admittance of the incident medium (SF10 glass prism in this case).

As proposed by Homola et al. [4], the propagation constant of a surface plasmon wave (SPW) propagating at the interface between a metal and dielectric sample can be written as

$$k_{\text{SPW}} = k\sqrt{\frac{\varepsilon_m n_{\text{sample}}^2}{\varepsilon_m + n_{\text{sample}}^2}}. \tag{10}$$

The real part of propagation constant of a SPW wave is given by

$$\text{Re}\left(k_{\text{SPW}}\right) \cong k\sqrt{\frac{\varepsilon_{mr} n_{\text{sample}}^2}{\varepsilon_{mr} + n_{\text{sample}}^2}}. \tag{11}$$

The coupling condition is given by

$$kn_{pr}\sin\theta_{\text{SPR}} = k\sqrt{\frac{\varepsilon_{mr} n_{\text{sample}}^2}{\varepsilon_{mr} + n_{\text{sample}}^2}}, \tag{12}$$

Table 1: Admittance and angle of incidence data for different alloy fractions.

Alloy film thickness (in nm)	Alloy fraction	Starting imaginary admittance	End admittance	Angle of incidence (in deg.)
45	0	$1.84i$	$1.801, -0.04842i$	56.36
44	0.5	$2.069i$	$1.736, -0.05507i$	55.31
43	1	$2.282i$	$1.715, -0.05429i$	54.59

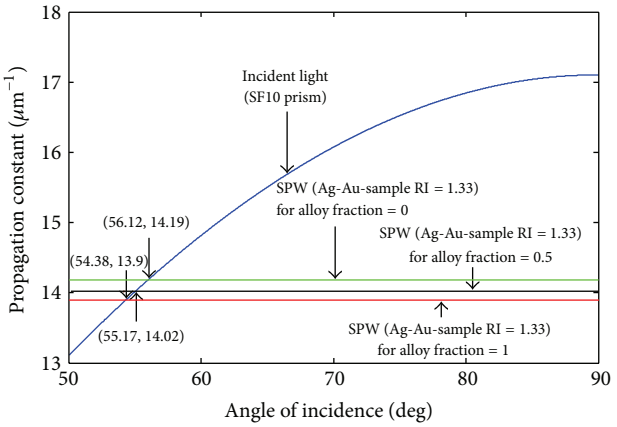

Figure 2: Plot of propagation constant of a plasmonic structure for Ag, Au metals and Ag-Au bimetallic alloy metal films, respectively.

where ε_m is the dielectric constant of the metal, ε_{mr} is the real part of dielectric constant of the metal, and k is the free space wave number.

The sensitivity of a plasmonic structure under consideration is given by [15]

$$S = \frac{d\theta_{\text{SPR}}}{dn_{\text{sample}}} = \frac{\left(\varepsilon_{mr}/\left(\varepsilon_{mr} + n_{\text{sample}}^2\right)\right)^{3/2}}{\sqrt{n_{pr}^2 - \left(\varepsilon_{mr} n_{\text{sample}}^2/\left(\varepsilon_{mr} + n_{\text{sample}}^2\right)\right)}}, \quad (13)$$

where $d\theta_{\text{SPR}}$ is the small change in SPR angle corresponding to small change in sample refractive index, dn_{sample}.

The detection accuracy (DA) of a plasmonic structure is given by

$$\text{DA} = \frac{1}{\text{FWHM}}, \quad (14)$$

where FWHM is the full width half maximum of SPR sensing curve.

3. Simulation Results and Discussion

3.1. Surface Plasmon Momentum Matching Condition. Figure 2 shows surface plasmon resonance condition for metals, namely, Ag (alloy fraction = 1), Au (alloy fraction = 0), and Ag-Au bimetallic alloy (alloy fraction = 0.5) with SF10 glass prism and sample RI of 1.33 at 633 nm wavelength. The intersections of curves correspond to propagation constant of incident light and propagation constant of surface plasmon wave that satisfy (12).

3.2. Admittance Loci Design Plots Based on Alloy Fraction Values. Figure 3(a) shows the admittance loci plot of silver (Ag) metal film with isoreflectance contours for SF10 glass prism and dielectric sample having refractive index (RI) 1.33 at 633 nm wavelength of light. Simulated admittance loci plot demonstrates that the starting admittance for the silver film is on the imaginary axis and the locus point moves from $2.282i$ on imaginary axis corresponding to silver film thickness of 0 nm to end at 1.715 on real axis corresponding to silver film thickness of 43 nm (which is close to refractive index of SF10 glass prism 1.72312, for an angle of incidence = 54.59°). It also corresponds to near-zero reflectance for that particular angle of incidence and silver metal film thickness. If we could have made this locus to intercept the real axis of the admittance diagram exactly at the refractive index of the incident medium (prism material) depending upon the metal film we are using (e.g., Au, Ag, etc.), the excitation of the surface plasmon would have been achieved with maximum efficiency. Similarly, in Figures 3(b) and 3(c), the admittance loci plots for Au metal film and Ag-Au bimetallic alloy film (alloy fraction value = 0.5 and nanoparticle size = 12 nm) have been shown.

The calculated values of starting and ending admittances and incident angles are tabulated in Table 1. In all these cases, we have optimized the bimetallic alloy film thicknesses so as to ensure the respective loci end with real admittance close to the value of refractive index of the prism to ensure efficient excitation of surface plasmons.

3.3. Admittance Loci Design Plots Based on Nanoparticle Size Variation. Figures 4(a) and 4(b) show admittance loci plots of a plasmonic structure for two different nanoparticle sizes of 10 nm and 14 nm, respectively, for a fixed Ag-Au alloy fraction value of 0.5.

Table 2 shows the calculated data of admittances and incident angles from simulated results of Figures 4(a), 3(c), and 4(b) for three different nanoparticle sizes (Ag-Au alloy film thickness = 44 nm).

3.4. Surface Plasmon Sensing Curves. Figure 5(a) shows the SPR sensing curves for Au (which corresponds to alloy fraction of 0) and Ag (which corresponds to alloy fraction of 1) metals in single plot, and Figure 5(b) shows SPR sensing curves for Ag-Au bimetallic alloy films of three different alloy fraction values as indicated in legend of the figure. Here the sample refractive index (RI) value is kept at 1.33 and the nanoparticle size is kept at 12 nm for both metals Ag and Au. Ag-Au alloy bimetallic film thickness is kept at 44 nm for alloy fraction values of 0.25 and 0.5, whereas the Ag-Au bimetallic

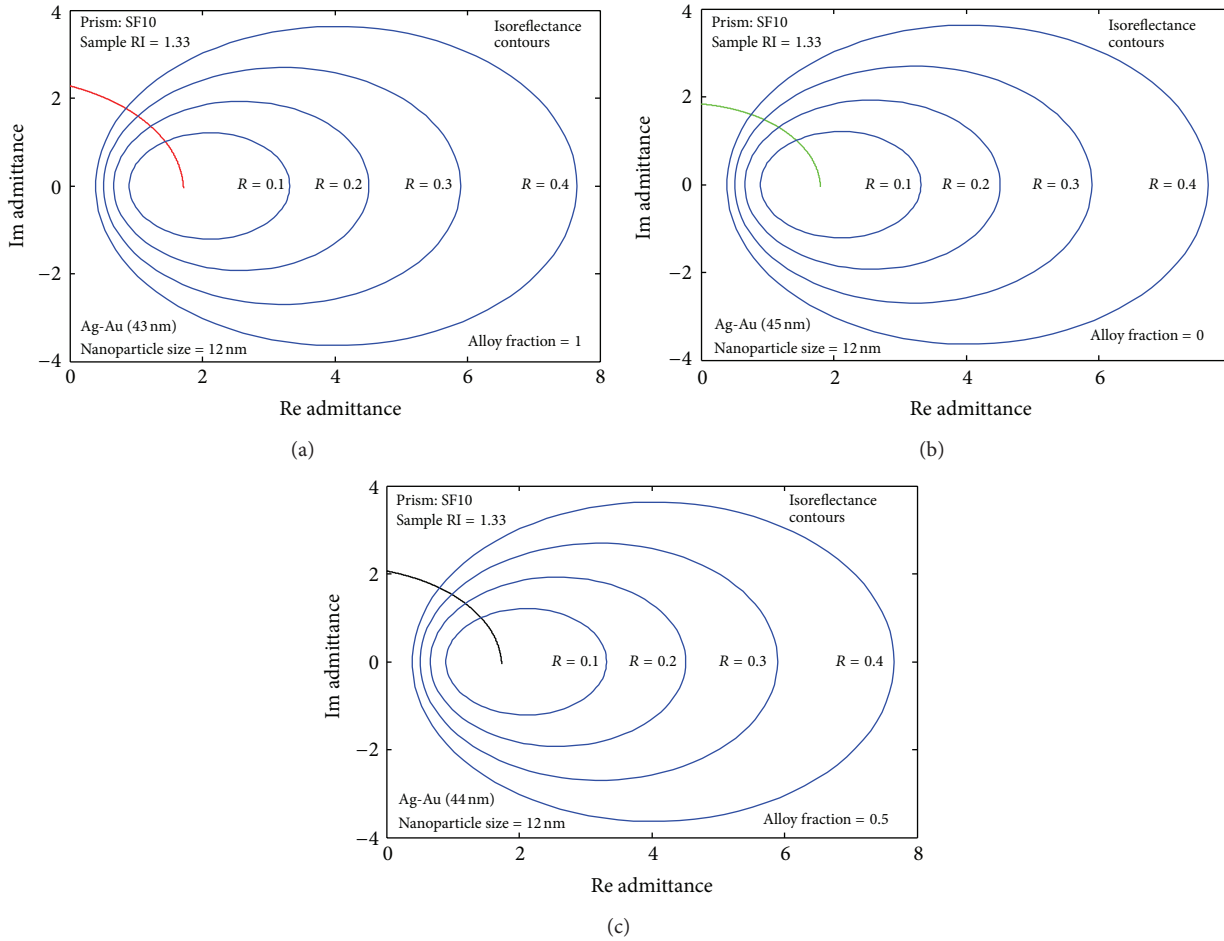

Figure 3: Admittance loci plot of a plasmonic structure for (a) silver film (alloy fraction = 1), (b) gold film (alloy fraction = 0), and (c) Ag-Au alloy film for alloy fraction of 0.5.

Table 2: Admittance and angle of incidence data for different nanoparticle sizes.

Alloy film thickness (in nm)	Nanoparticle size (in nm)	Starting imaginary admittance	End admittance	Angle of incidence (in deg.)
44	10	$2.066i$	$1.781, -0.1837i$	55.32
44	12	$2.069i$	$1.736, -0.05507i$	55.31
44	14	$2.072i$	$1.706, 0.04438i$	55.30

alloy film thickness is kept at 43 nm for alloy fraction values of 0.75 and 1 in order to obtain minimum reflectance. In both of the above-mentioned cases, the metal nanoparticle size is kept at 12 nm. Figure 5(c) shows SPR sensing curves for three nanoparticle sizes of 10 nm, 12 nm, and 14 nm, respectively, with a fixed value alloy fraction value of 0.5. From our simulated curves, it is seen that for a fixed nanoparticle size of 12 nm, SPR dip position shifts are more prominent and clearly distinguishable with change in alloy fraction values, whereas for a fixed alloy fraction of 0.5, SPR dip position shifts are less prominent with change in nanoparticle size.

3.5. Performance Parameters Considerations. The sensitivity can be theoretically evaluated using (13). The full width half maximum (FWHM) is an important factor to be considered for the actual design of a plasmonic structure. Another important parameter is the dynamic range which is defined as the range of dielectric samples which can be sensed as governed by surface plasmon resonance condition. The maximum value of the refractive index of the sample that can be sensed by a particular plasmonic structure can be obtained using (12) for which $\sin(\theta_{SPR})$ is just less than 1 [15]. For Au metal (Au nanoparticle size = 12 nm), the sample refractive index for which $\theta_{SPR} = 90^{\circ}$ was calculated to be $(n_{sample})_{max} = 1.5545$. So, with Au metal having nanoparticle size of 12 nm and SF10 glass prism at 633 nm wavelength, all the dielectric samples with refractive indices less than 1.5545 are detectable. Table 3 shows the values of dynamic

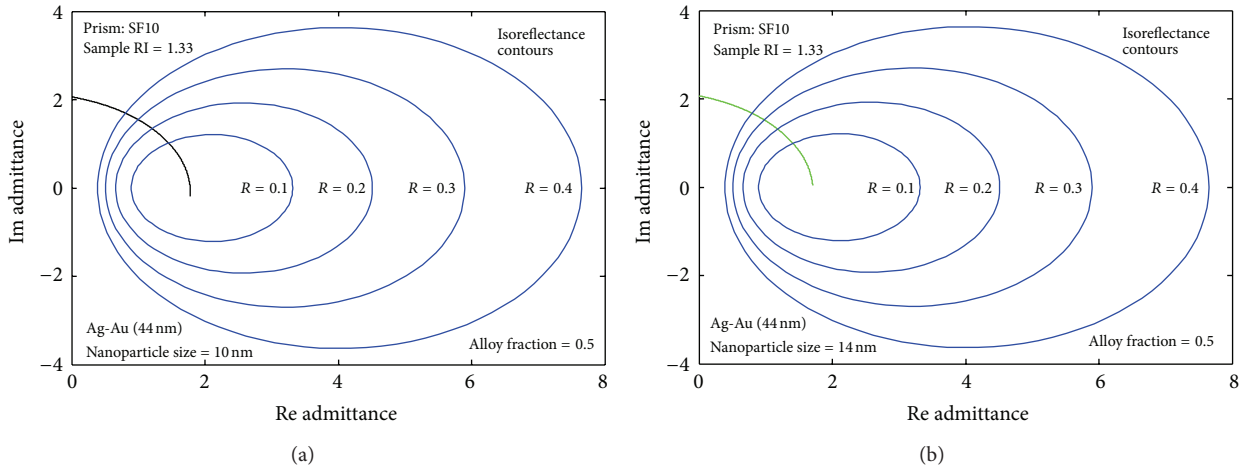

FIGURE 4: Admittance loci plot for nanoparticle sizes of (a) 10 nm and (b) 14 nm.

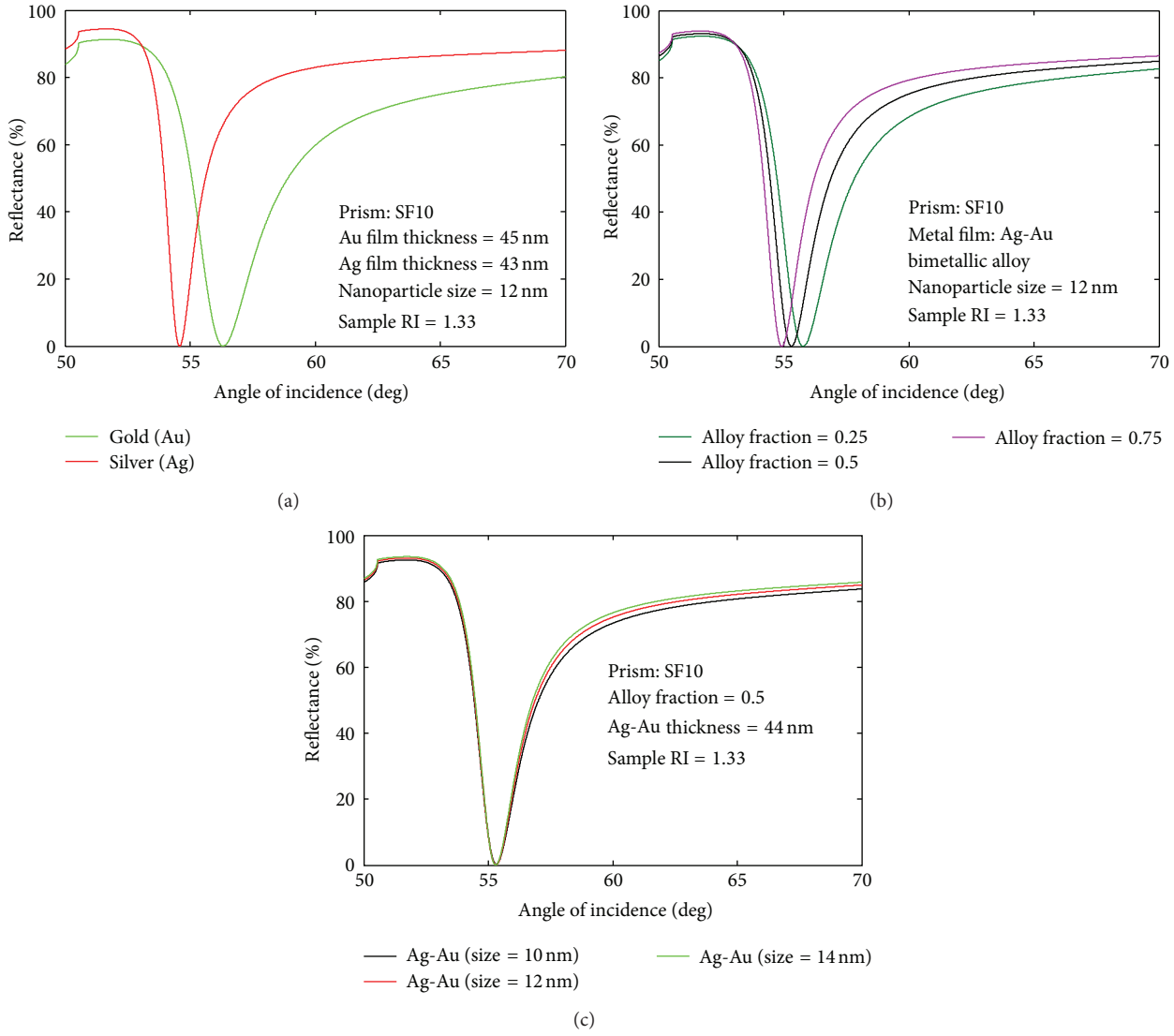

FIGURE 5: SPR curves of a plasmonic structure using (a) silver and gold metal films, (b) Ag-Au alloy film for three different alloy fractions of 0.25, 0.5, and 0.75, with fixed nanoparticle size of 12 nm, and (c) Ag-Au alloy film for three different nanoparticle sizes of 10 nm, 12 nm, and 14 nm, with fixed alloy fraction of 0.5.

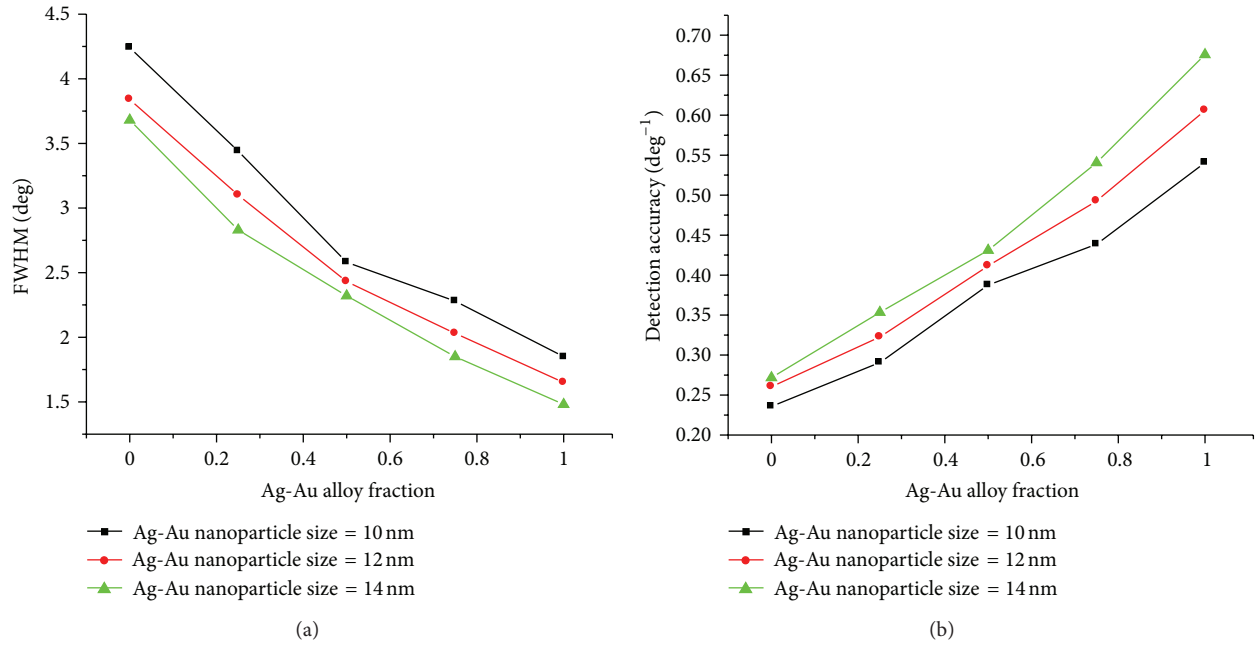

Figure 6: Plot of (a) FWHM and (b) detection accuracy versus alloy fraction values of bimetallic film with sample RI = 1.33 for three different metal nanoparticle sizes.

Table 3: Calculated values of dynamic range, SPR angle, and sensitivity.

Alloy fraction	Ag-Au alloy films								
	Nanoparticle size = 10 nm			Nanoparticle size = 12 nm			Nanoparticle size = 14 nm		
	Dynamic range	SPR angle (deg.)	Sensitivity (deg./RIU)	Dynamic range	SPR angle (deg.)	Sensitivity (deg./RIU)	Dynamic range	SPR angle (deg.)	Sensitivity (deg./RIU)
0	1.5542	56.36	74.4581	1.5545	56.34	74.3996	1.5547	56.33	74.3605
0.25	1.5668	55.81	71.9072	1.5670	55.79	71.8621	1.5672	55.76	71.8321
0.5	1.5776	55.32	69.8846	1.5778	55.31	69.8489	1.5780	55.3	69.8253
0.75	1.5871	54.95	68.2413	1.5872	54.93	68.2124	1.5873	54.91	68.1935
1	1.5953	54.61	66.8797	1.5955	54.59	66.8559	1.5956	54.57	66.8404

range, SPR angle, and sensitivity of the structure, and it is seen from the data provided in table that as the alloy fraction value increases, the dynamic range increases. Moreover, for bigger nanoparticle size, the value of dynamic range is higher than that for smaller nanoparticle size, whereas SPR angle and sensitivity are found to decrease with increase in alloy fraction values. It is also seen that higher value of nanoparticle size in alloy film shows lowest sensitivity and using lower value of nanoparticle size ensures highest sensitivity. So one should choose the correct value of Ag-Au bimetallic alloy fraction and nanoparticle size depending on the application concerned with a compromise between the sensitivity and the dynamic range.

3.6. Nanoparticle Size Dependency. Figures 6(a) and 6(b) show the plot of variation of full width half maximum (FWHM) and Detection accuracy with alloy fraction values for three different nanoparticle sizes under consideration, namely, 10 nm, 12 nm, and 14 nm, respectively. It can be concluded that FWHM decreases as alloy fraction value increases, whereas detection accuracy increases with increase in alloy fraction values for a fixed nanoparticle size in both cases. It is also clear that FWHM is higher for smaller nanoparticle size and lower for bigger nanoparticle size and vice versa in case of detection accuracy. So using bigger nanoparticle size ensures precise SPR dip position determination for more accurate SPR sensing.

4. Conclusion

We have theoretically investigated the Ag-Au bimetallic alloy fraction and nanoparticle size dependency of a plasmonic structure using admittance loci method. In this work, we have used different alloy fractions and nanoparticle sizes of Ag-Au bimetallic alloy film in order to see the effect of these parameters on admittance loci plots of the plasmonic structure and also on SPR sensing curves. We have also studied various parameters related to SPR sensing, namely,

SPR angle, sensitivity, dynamic range, FWHM, and detection accuracy. These parameters are found to be influenced by the different alloy fraction values and nanoparticle sizes of Ag-Au bimetallic alloy film used. The choice of alloy fraction value and nanoparticle size of Ag-Au bimetallic alloy film must be in accordance with the application concerned keeping in mind the optimized tradeoff between the sensitivity, FWHM, and dynamic range requirements.

Conflict of Interests

The authors declare that there is no conflict of interests regarding the publication of this paper.

Acknowledgments

The authors wish to acknowledge the support of Centre for Research in Nanoscience and Nanotechnology (CRNN), University of Calcutta, Kolkata, India. Kaushik Brahmachari is grateful to Technical Education Quality Improvement Programme (TEQIP PHASE II), University College of Technology, University of Calcutta, for awarding Senior Research Assistantship to carry out this work.

References

[1] A. Otto, "Excitation of nonradiative surface plasma waves in silver by the method of frustrated total reflection," *Zeitschrift für Physik*, vol. 216, no. 4, pp. 398–410, 1968.

[2] E. Kretschmann and H. Raether, "Radiative decay of nonradiative surface plasmons excited by light," *Zeitschrift für Naturforschung*, vol. 23, pp. 2135–2136, 1968.

[3] B. Liedberg, C. Nylander, and I. Lunström, "Surface plasmon resonance for gas detection and biosensing," *Sensors and Actuators*, vol. 4, pp. 299–304, 1983.

[4] J. Homola, I. Koudela, and S. S. Yee, "Surface plasmon resonance sensors based on diffraction gratings and prism couplers: sensitivity comparison," *Sensors and Actuators B*, vol. 54, no. 1, pp. 16–24, 1999.

[5] K. Brahmachari and M. Ray, "Modelling of chalcogenide glass based plasmonic structure for chemical sensing using near infrared light," *Optik*, vol. 124, no. 21, pp. 5170–5176, 2013.

[6] K. Brahmachari and M. Ray, "Performance of admittance loci based design of plasmonic sensor at infrared wavelength," *Optical Engineering*, vol. 52, no. 8, Article ID 087112, 2013.

[7] S. Ghosh, K. Brahmachari, and M. Ray, "Experimental investigation of surface plasmon resonance using tapered cylindrical light guides with metal-dielectric interface," *Journal of Sensor Technology*, vol. 2, no. 1, pp. 48–54, 2012.

[8] H. A. Macleod, *Thin-Film Optical Filters*, Taylor & Francis Group, New York, NY, USA, 4th edition, 2010.

[9] C.-W. Lin, K.-P. Chen, M.-C. Su, C.-K. Lee, and C.-C. Yang, "Bio-plasmonics: nano/micro structure of surface plasmon resonance devices for biomedicine," *Optical and Quantum Electronics*, vol. 37, no. 13–15, pp. 1423–1437, 2005.

[10] C.-W. Lin, K.-P. Chen, M.-C. Su et al., "Admittance loci design method for multilayer surface plasmon resonance devices," *Sensors and Actuators B*, vol. 117, no. 1, pp. 219–229, 2006.

[11] C.-W. Lin, K.-P. Chen, C.-N. Hsiao, S. Lin, and C.-K. Lee, "Design and fabrication of an alternating dielectric multi-layer device for surface plasmon resonance sensor," *Sensors and Actuators B*, vol. 113, no. 1, pp. 169–176, 2006.

[12] Y.-J. Jen, A. Lakhtakia, C.-W. Yu, and T.-Y. Chan, "Multilayered structures for p- and s-polarized long-range surface-plasmon-polariton propagation," *Journal of the Optical Society of America A*, vol. 26, no. 12, pp. 2600–2606, 2009.

[13] K. Brahmachari, S. Ghosh, and M. Ray, "Surface plasmon resonance based sensing of different chemical and biological samples using admittance loci method," *Photonic Sensors*, vol. 3, no. 2, pp. 159–167, 2013.

[14] K. Brahmachari and M. Ray, "Effect of prism material on design of surface plasmon resonance sensor by admittance loci method," *Frontiers of Optoelectronics*, vol. 6, no. 2, pp. 185–193, 2013, Erratum in: Frontiers of Optoelectronics, vol. 6, no. 3, pp. 353, 2013.

[15] G. Gupta and J. Kondoh, "Tuning and sensitivity enhancement of surface plasmon resonance sensor," *Sensors and Actuators B*, vol. 122, no. 2, pp. 381–388, 2007.

[16] A. K. Sharma and G. J. Mohr, "On the performance of surface plasmon resonance based fibre optic sensor with different bimetallic nanoparticle alloy combinations," *Journal of Physics D*, vol. 41, no. 5, Article ID 055106, 2008.

[17] R. Jha and A. K. Sharma, "Chalcogenide glass prism based SPR sensor with Ag-Au bimetallic nanoparticle alloy in infrared wavelength region," *Journal of Optics A*, vol. 11, no. 4, Article ID 045502, 2009.

[18] A. K. Sharma and R. Jha, "Surface plasmon resonance-based gas sensor with chalcogenide glass and bimetallic alloy nanoparticle layer," *Journal of Applied Physics*, vol. 106, no. 10, Article ID 103101, 2009.

[19] A. K. Sharma and B. D. Gupta, "Fibre-optic sensor based on surface plasmon resonance with Ag-Au alloy nanoparticle films," *Nanotechnology*, vol. 17, no. 1, pp. 124–131, 2006.

[20] A. K. Sharma and B. D. Gupta, "Comparison of performance parameters of conventional and nano-plasmonic fiber optic sensors," *Plasmonics*, vol. 2, no. 2, pp. 51–54, 2007.